Noname manuscript No.
(will be inserted by the editor)

Studies on the materials of LARES 2 satellite

A. Paolozzi · G. Sindoni · F. Felli · D. Pilone · A. Brotzu · I. Ciufolini · E. C. Pavlis · C. Paris

Received: date / Accepted: date

Abstract LARES 2 is an Italian Space Agency (ASI) satellite designed for testing with unprecedented accuracy frame-dragging, a fundamental prediction of General Relativity, and to contribute to space geodesy with a precision higher than any other satellite presently in orbit. The choice of the material for the body of LARES 2 satellite determines, along with its dimensions, the surface-to-mass ratio minimization which is the main requirement for the satellite. The paper will report the studies conducted for the fulfilment of the above mentioned requirement and the tests performed to qualify the materials for construction of the the satellite.

Keywords LARES 2 · Frame–dragging · Lense–Thirring effect · Nickel and Copper alloys · fused silica · PCTFE

A. Paolozzi, G. Sindoni
Scuola di Ingegneria Aerospaziale
Sapienza Università di Roma
E-mail: giampiero.sindoni@uniroma1.it

F. Felli, D. Pilone, A. Brotzu
DICMA, Sapienza Università di Roma

I. Ciufolini
Universita del Salento
Dipartimento di Ingegneria dell'Innovazione

E. C. Pavlis
Joint Center for Earth Systems Technology, (JCET/UMBC)
University of Maryland, BC & NASA Goddard

C. Paris
Centro Fermi – Museo Storico della Fisica
e Centro Studi e Ricerche "Enrico Fermi", Rome, Italy

1 Introduction

LARES 2 is a follow-on mission of the LARES (LAser RElativity Satellite) satellite launched in 2012 [1] having the same main objective but with a much higher accuracy: the measurement of a General Relativity phenomenon called frame-dragging due to the Earth rotation [2] with an accuracy improved by one order of magnitude with respect to LARES. Besides its contribution to General Relativity, LARES 2 will also provide other measurements in fundamental physics, as provided by LARES [3] and in geodesy and environmental monitoring [4]. Back in 1986 and 1989 an idea was published on how to make such a measurement using passive satellites [5,6]. In 1998, the LARES satellite was first presented and described in some papers [7] but the first real launch opportunity was given in 2008 when the new VEGA launcher of ESA was in an advanced state of development by ELV (an Avio-ASI joint venture). The capability of VEGA with a payload of 700 kg were limited to about 1500 km, so that the approach proposed in [5,6] was used: three satellites essentially at very high altitude orbit can be exploited to eliminate the uncertainties in the first two even zonal harmonics, thus allowing to reach an accuracy of a few percent in the frame dragging measurement as shown by the simulations reported in [8]. The upcoming LARES 2 satellite will have a supplementary orbit with respect to LAGEOS 1 allowing the removal of all the uncertainties due to the even zonal harmonics of the terrestrial gravity field. LARES 2 satellite will be released in orbit without any spin.

The *dragging of inertial frames* [12–15], or *frame-dragging* as Einstein called it in 1913 [16], is an intriguing and fascinating prediction of General Relativity. The axes of the inertial frames (locally) are not fixed with respect to the distant stars (i.e., with respect to an asymptotic inertial frame) but they are dragged by the mass-energy currents. Indeed local gyroscopes define the axes of the local inertial frames and they are not fixed with respect to the distant stars (as in classical mechanics) but they are dragged by mass-energy currents, such as the angular momentum of a central body, in a way formally similar, in weak-field and slow-motion, to the change of orientation of a magnetic dipole (Larmor precession) due to the magnetic moment of a central electric current. For this formal analogy with electrodynamics, frame-dragging was also called *gravitomagnetism*. Frame-dragging has a key role in a number of fundamental phenomena of General Relativity and high energy astrophysics. The generation of gravitational waves emitted by the collision of two spinning black holes forming a spinning black hole, such as the gravitational waves measured by LIGO [17], involves frame-dragging and thus the basic computer simulations of such collisions must include frame-dragging. Furthermore, the constant orientation of the gigantic jets emitted by quasars and active galactic nuclei, over periods that may reach millions of years, is explained by the gravitomagnetic field of a central spinning black hole [17]. Frame-dragging was measured in 2004-2010 using the LAGEOS and LAGEOS 2 satellites [9,10], with an accuracy of about 10% and in 2016, using the LARES, LAGEOS and LAGEOS 2 satellites [11], with an accuracy of about 5%. The forthcoming

LARES 2 satellite, together with the LAGEOS satellite, will measure it with an accuracy of a few parts in a thousand [18–22] .

2 The satellite

Unlike LAGEOS 2, that is a copy of LAGEOS 1 (there are only small differences between the two), LARES 2 is rather different from LARES satellite [22]. To begin with, the altitude of the two orbits is quite different (1450 km for the first and 5890 for the second). The satellite body is made in one single block as LARES [23] but with a larger size and different material. The CCRs are more densely packed in the LARES 2 design and are 1 inch in diameter with no coating on back faces. This solution was chosen for all the LAGEOSs and LARES satellite to avoid additional thermal gradient on CCR. The average value of the experimental optical cross section, measured on a group of ten LARES 2 CCRs has been 0.358 $\pm$ 0.026 (1-σ) 10^6 m^2 . The mean value of Dihedral angle offset (DAO) measured on ten samples is 0.34" $\pm$ 1.06" (1-σ). In Table 1 we list key parameters of some laser ranged satellites with the lowest surface-to-mass ratio. The final radius of LARES 2 is strictly related to the final material that will be used for the body of the satellite [24] and it is in the range listed in Table 1.

Currently there are two families of alloys under investigation. The first one, Copper alloy, has high thermal conductivity that could ultimately reduce thermal thrust [25,21], a tiny but not negligible perturbation on laser ranged satellites. The second one, a nickel alloy, which is the baseline, is more convenient from the point of view of the mechanical characteristics that are quite demanding at the interfaces with the separation system [26]. The thermo-optical properties of the two materials is another aspect to take into account for the final choice because the satellite temperature is strongly dependent on the values of emissivity and absorptivity of the material [27].

Table 1 Comparison of LARES 2 with some other laser ranged satellites

	LAGEOS	LAGEOS 2	LARES	LARES 2	Starlette	Stella
Perigee [Km]	5890	5620	1450	5890	812	804
Eccentricity	0.0045	0.0125	0.0008	0.0025	0.0206	0.0206
Inclination	109.84^o	52.64^o	69.5^o	70.16^o	48.83^o	98.36^o
Diameter [mm]	600	600	364	404-424[1]	240	240
No. of CCR	426	426	92	∼303	60	60
Mass [Kg]	406.9	405.3	386.8	280–300[1]	47.5	48
Mass/Cross Section wrt LAGEOS	1	0.99	2.6	1.46–1.51[1]	0.73	0.72
Theoretical Optical c.s. [10^6 m^2]	15	15	3.3	3.9-4.2		

One requirement for LARES 2 is to adapt the CCR distribution in such a way to accommodate the interfaces with the separation system used for

[1] Actual values will depend upon the final alloy selected.

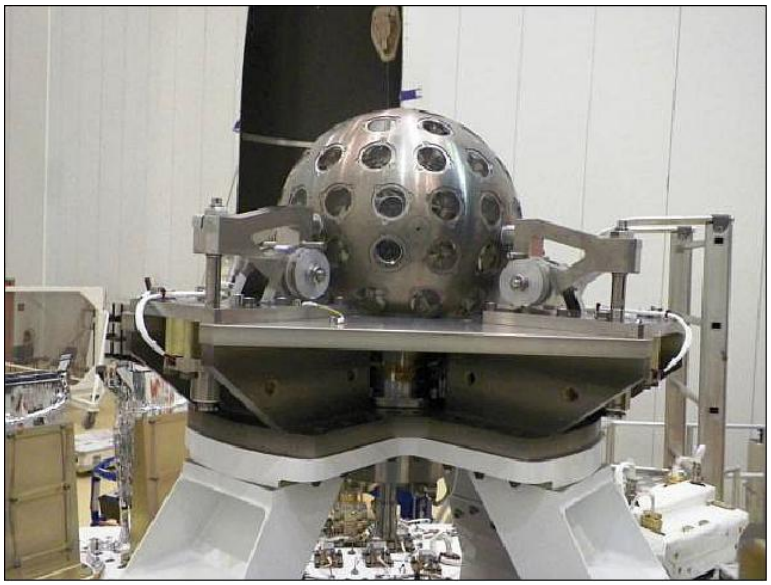

Fig. 1 LARES satellite on the separation system (image credit: ASI).

LARES [28]. Figure 1 shows LARES satellite mounted on the separation system and it is possible to see two of the four supporting arms of the separation system. Each of the four arms applied 26612 N to the LARES hemispherical cavity. Only small variations due to the different diameter of LARES 2 compared to LARES are allowed. This approach will reduce the cost and above all the manufacturing time which is a critical parameter for the LARES 2 mission schedule. The design values of the forces applied separately by each single arm to LARES 2 have increased with respect to LARES to a value of 35 kN. Figure 2 shows two curves, one representing the maximum pressures calculated at the contact area in the hemispherical cavity and the other the required value of yield strength for the alloy to be chosen. The calculation was performed using the Hertz formula. The requirement have been estimated using a safety factor that accounted for the accuracy limit of the Hertz formula and the ECSS regulation. The curves show rhe stress as a function of the elastic modulus of the alloy and indicate that the higher the elastic modulus the higher the maximum value of the pressure. That is intuitively correct since a softer material will deform more, so that the total applied force will be distributed in a larger area thus reducing the local maximum of the pressure. Thermal tests analogous to the ones performed on a breadboard of LARES [29,30] are planned also on LARES 2 satellite.

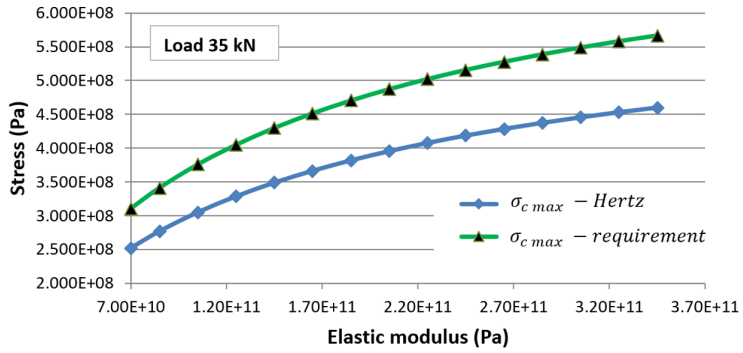

Fig. 2 LARES 2. Pressures at separation system interface, σ_c is the stress in the contact area.

3 Materials.

Similar to LARES satellite, there are only three different materials for LARES 2 satellite: the body, the caps, the screws and the retainer rings are made of one single metal alloy; the CCRs are made of fused silica and the plastics rings are made of PCTFE. The fused silica grade used for the LARES 2 CCRs is different from the one used for LARES (see specific section below), the metal has a density which is lower than that of LARES (tungsten). In the next three sections we present studies of the three different materials will be reported.

4 Metal alloy

The choice of the material dictates the fulfillment of the science requirements impacting on the satellite design and of the requirements imposed by the separation system. The first ones include the material density, magnetic permeability and thermo-optical properties; the second ones include the elastic modulus, the yield strength and the hardness. In addition to those important requirements a high thermal conductivity of the material is preferable. At the beginning of the design phase the mass budget was established in the range 320-350 kg. Adopting a tentative diameter of 0.4 m for the satellite the required density was in the range 9000-10000 kg/m^3. Therefore, the candidate alloys with reasonable price were Copper, Nickel and Cobalt based. An austenitic stainless steel was also considered for its good mechanical characteristics and for being also nonmagnetic, but the density needed to by increased. We started with the Inconel family because all the alloys of this group, with the exclusion of Inconel 783, guarantee an elastic modulus greater than 200 GPa as required by the separation system. The yield strength is required to be higher than 517 MPa. According to the data sheets (see [31]) most of the Inconel alloys, with the exclusion of the Inconel 686, C-276, HX and N06230, fulfill also this requirement. In Table 2 and Table 3 we list the compositions,

Fig. 3 Ingot of the varied Inconel 600 alloy: ingot inside the graphite mold (Left) and after extraction from the mold (Right).

densities and elastic moduli of all the Inconel alloys. The value of the yield strength is not reported in the table because it varies largely depending on the manufacturing process of the ingot and thermal treatment. With the exclusion of the four alloys mentioned above it can be certainly identified a production process and thermal treatment that fulfill the requirement. Unfortunately, the alloys with the highest densities i.e. the Inconel 686 (8730 kg/m^3), C-276 (8890 kg/m^3) and N06230 (8910 kg/m^3), do not fulfill the yield requirement. We also observed that those alloys are the only ones with tungsten (W) in the composition (alloy Inconel HX has W but with a content less than 1%). It is therefore reasonable to assume that the cause for the high value of density as well as the lower yield is the presence of W with content higher than 3%. Of course, a more detailed study supported by experimental realization of small ingots is required to confirm this hypothesis. Anyway, we decided, based on the previous considerations, to avoid the use of W in the modified versions of Inconel alloys that we realized. Excluding the four Inconel alloys that do not meet the yield requirement, the one that has the higher density is the Inconel 600 with a value of 8470 kg/m^3. The density of this alloy was below the target thus calling for the modification in the composition. A heavier element was required and the only one, besides W, that is already used in other Inconel alloys with significant percentage was Molybdenum that is very soluble in Nickel. We realize the alloy with the addition of 20% of Molybdenum, with a corresponding reduction of Nickel, and a reduction of Cr at 13% just below the lower limit of 14% of the Inconel 600. The alloy was cast twice in vacuum using a centrifugal induction furnace (Figure 3). The Energy Dispersion Spectroscopy (EDS) analysis has provided for the two specimens, referred to as Ni-1A and Ni-1B, small variations in the composition with respect to the chosen nominal composition (fourth column of Table 4) of the varied Inconel 600 alloy. The densities calculated with weight averaging of the two specimens were 8812 kg/m^3 and 8890 kg/m^3 while the experimental value was slightly lower (8700 kg/m^3). Those values of densities were at the lower end of the requirement and so the option of Inconel was considered a good one but the studies for other

options continued. We noted that the density estimation by weight average of the elements can be used only as a very rough indication: in fact, only the realization of ingots can confirm the actual value of the density, which is affected by several factors. The difference in the density estimation can be higher than that found earlier like in the case of a Cobalt (Co) alloy commercialized under the name of Haynes 188. The density calculated with the weight average of the elements of this alloy provided a value of 9908 kg/m^3, while the value of the producer is lower and equal to 8980 kg/m^3 (see for instance [32]). We also cast an ingot of the Haynes 188 with the composition reported in the last two columns of Table 4. Again, we found an actual density lower than the theoretical one. Further studies on this alloy were not carried out because it was found the alloy to be magnetic. One possible explanation of the deviation from the expected density is that the mixing of the elements can deform the crystal lattice in such a way to change the density of the alloy. The biggest change was observed in the alloys containing W. More difficult is the situation with the Copper alloys that for sure cannot fulfill the requirement of 200 GPa of the elastic modulus since any Copper alloy has values in the range 110-130 GPa. This requirement indeed is not so strict and could be relaxed because a lower value of the elastic modulus, according to Fig. 2 will reduce the yield strength to about 410 MPa. This reduction will make it easier to find a Copper alloy for LARES 2 satellite. The main problem remains the surface hardness that it is difficult to reach with Beryllium free Copper alloys. Copper alloys are attractive for LARES 2 because of their very high thermal conductivity which can be up to 30 times that of a Nickel (Ni) alloy. The high thermal conductivity will make the surface temperature of the satellite more uniform thus reducing the thermal thrust perturbation, although this effect may be mitigated by the presence of the eclipses. Lowest thermal trust and best behavior of the CCRs are possible selecting the combination between alloy and surface finishing, that minimize the absorbtivity to emissivity ratio. So for the design purpose there is no need of thermal analysis not even a transient analysis since the specific heat of the alloys under consideration is pratically the same. Of course the estimation of the thermal trust based on thermovacuum tests and orbital analysis will be performed. On the other hand, Copper is more reactive to oxidation than a Ni or Co based alloy. Consequently after manufacturing and before the launch, the atmosphere can change the thermo-optical properties of the surface, if no special actions are taken. To avoid surface oxidation on the copper alloy, soon after satellite manufacturing and cleaning, a thin plastic film is applied on the satellite surface. The integration of the satellite is performed in clean room, after removal of the film, with controlled humidity condition, the transfer of the integrated satellite to the launch site will be performed in transport container with N2 controlled atmosphere. In Ref. [33] more detailed analysis on Copper alloys composition, density and hardness is reported. The alloys were divided into three groups (see Fig. 4: cupronickel (gray), bronze (brown) and brass (orange). Most of those alloys report densities around 9000 kg/m^3.

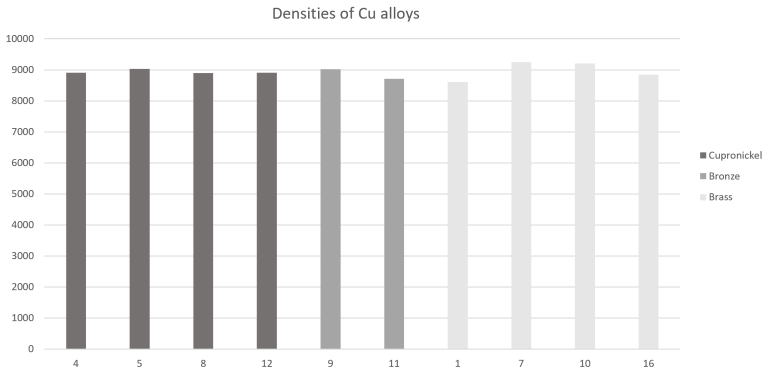

Fig. 4 Copper alloy densities, cupronickel (gray), bronze (brown) and brass (orange).

Unfortunately, the maximum value of hardness, obtained with a brass alloy (composition: Cu balance, Ni 5.3%, Si 0.5%, Ag 9.3%, Pb 6.6, Zn 9.9; 5 h aging at 500 ^{o}C), was 223 HV10 (corresponding to about 20 HRC) well below the requirement. The presence of Silver (Ag) and Zinc (Zn) in the composition was an attempt to reduce the absorptivity-to-emissivity ratio decided based on some tests performed in thermovacuum with Zn and Ag alloys. The composition was also chosen in such a way to allow the age hardening due to the formation of Ni_2Si precipitates. The fact that the hardness did not improve significantly may be due to the presence of Lead (Pb), this aspect can be investigated in a future study. The conclusion that can be drawn from those experimental results is that those alloys could be used for the satellite only if inserts of different metals with the appropriate characteristics are used on the satellite in correspondence of the separation system interface, but this artifice represents a manufacturing complication. We therefore have continued to study other beryllium free Copper alloys that could be precipitation hardened to obtain the yield and hardness required. We have selected two commercial alloys C19500 and C70250 that, according to the datasheet, would have met the yield requirement. However, data on hardness were not available, consequently we manufactured several ingots, at the Centro Sviluppo Materiali (CSM) in Castel Romano (Rome, Italy) using Vacuum Induction Melting (VIM). The alloy C19500 resulted magnetic and so it was discarded, the alloy C70250 has been studied in detail and results are reported in [24]. The composition of the alloy has been slightly modified to improve the hardening process during aging, in particular the Ni has been increased to 5% (maximum for the alloy is 4.2%) and Mg to 0.6% (maximum for the alloy is 0,3%). In fact the alloy reached both the yield and hardness requirement with an aging performed in the range 8h to 16h. At shorter aging time the precipitation was not enough and at longer aging time, the hardness decreased due to overaging. The density of the commercial alloy is 8800 kg/m^3 while the one produced at CSM is 8970 kg/m^3. The advantages of this alloy are: the fulfillment of all the requirements with the exclusion of the elastic modulus, lower cost than nickel alloys, higher

Fig. 5 Optical micrograph of Copper alloy 206 (Metalminotti S.r.l.) after annealing and aging (chemical etching: ferric chloride).

thermal conductivity and faster manufacturing of the finished part. However, procuring of about 500 kg in single block of this alloy needed a long experimentation. A similar alloy is under experimentation at Metalminotti S.r.l. with the commercial name Alloy 206. We have performed an experimental characterization of the alloy (that at the moment is confidential and cannot be completely disclosed). The yield of the bar as received, i.e. annealed, rolled and aged has a yield higher than the requirement and a hardness almost reaching the requirement. With a more specific heat treatment the hardness reached a value slightly higher than the requirement. The characterization implied the manufacturing of several specimens both for tensile tests and hardness tests. Different specimens were subjected to different thermal treatments before the tensile and hardness test were performed. This was important to establish for instance the aging time required to fulfill the requirements. Besides the mechanical characterization, similarly to what done to all the other alloys, also a microstructure analysis was performed. The Alloy 206 after aging, shows a different phase, indicated by the arrows (Figure 5) that analyzed by means of EDS seems to be an eutectic component (Cr-Cr_3 Si). It is under investigation whether this phase can be a problem for manufacturing a large size block of material. A further study was performed on a Ni(67%)-Mo(25%)-Cr(8%) alloy commercialized as Haynes 242. This alloy has been tested using both a commercial rod and ingots produced at CSM. Unlike the Copper alloy the hardening process needed to be longer but no overaging phenomena have been observed up to 120 h of thermal treatment performed at 650°C. The density of the alloy is in the range 9050-9070 kg/m^3. The Young's modulus ranges

from 220 to 230 GPa, the yield strength and hardness requirement is fulfilled with the aged alloy. Depending on the melting process and forging used, the duration of aging required to fulfill the requirements may vary in the range 24h-120h. From any family of the alloys analyzed, a screw and a female screw were manufactured to test the machinability of the alloys. The tests were successful for all the alloys and, as expected, the nickel alloys required specific tools and longer manufacturing time. In conclusion there are several possible alloys that can be used for manufacturing LARES 2 satellite. The nickel alloys guarantee the highest stability with respect to surface thermo-optical change due to air before the launch, high yield strength, elastic modulus and hardness. Also, with nickel alloys different surface finish have less effect on the variations of the thermo-optical properties. These alloys come in a wide range of different densities, enabling flexibility in the alloy selection with the variation of the satellite's size or the mass budget made available by the launcher. Among the analyzed alloys, the one fulfilling all the mechanical requirements and with the highest density is the one commercialized under the name of Haynes 242. On the other hand, thermal conductivity of all nickel alloys considered is low and manufacturing harder than Copper alloys. If one accepts an additional complication in the mechanical design of the body of the satellite, implying the use of inserts of a different material at the separation system interface, also Copper alloys provide a wide range of possibilities. If the inserts are not the preferred solution, then the choice of the alloy (Beryllium free) can fall on the C70250 or on limited variations of it. These types of alloys have a Ni content of about 5% and about 1% of Si that allow to reach the mechanical requirement with a proper aging time and temperature. An important aspect for the choice of the alloy will be the procuring time for the semifinished product. That is due to the short time to launch that is foreseen at the end of 2019 or at 2020. The wide range of possible alloys described above makes this last aspect not so critical.

Table 2 Inconel alloy composition (in % weight), density and elastic modulus. (*) including cobalt, (**) including tantalum

Inconel alloy	600	601	617	625	686	690	693	718
Density (Kg/m^3)	8470	8110	8360	8440	8730	8190	7770	8190
Ni	72(*)	58-63	44.5 min	58 min	Bal.	58 min.	Bal.	50-55(*)
Co			10.0-15.0	1.0 max				1 max
Cr	14-17	21-25	20-24	20-23	19-23	27.0-31	27-31.0	17-21.0
Fe	6.0-10.0	Bal.	3 max	5 max	2 max	7-11	2.5-6.0	Bal.
Mn	1.0 max	1.0 max	1.0 max	0.5 max	0.75	0.5 max	1 max	0.35 max
Cu	0.5 max	1.0 max	0.5 max			0.5 max	0.5 max	0.30max
Si	0.5 max	0.5 max	1.0 max	0.5 max	0.08 max	0.5 max	0.5 max	0.35 max
Mo			8.0-10	8-10.0	15-17			2.8-3.3
Nb				3.15-4.15*			0.5-2.5	4.75-5.5
Ti			0.6 max	0.4 max**	0.02-0.25		1 max	0.65-1.15
Al			0.8-1.5	0.4 max			2.5-4.0	0.2-0.8
W					3-4.4			
C	0.15 max.	0.1 max.	0.05-0.15	0.1 max	0.01 max	0.05 max	0.15 max	0.08 max
Elastic modulus (GPa)	214	206.5	211	204.8-207.5	207	211	196	200

Table 3 Continuation of Table 2

Inconel Alloy	725	740	751	783	C-276	HX	N06230	X-750
Density (kg/m^3)	8310	8050	8220	7810	8890	8200	8910	8280
Ni	55-59	Bal.	70.0 min.	26.0-30.0	Bal.	Bal.	Bal.	70.0 min.
Co		20.0	–	Bal.	2.5 max.	0.5-2.5	5.0 max.	1.0 max.
Cr	19-22.5	25.0	14.0-17.0	2.5-3.5	14.5-16.5	20.5-23.0	20.0-24.0	14.0-17.0
Fe	Bal.	0.7	5.0-9.0	24.0-27.0	4.0-7.0	17.0-20.0	3.0 max.	5.0-9.0
Mn	0.35 max.	0.3	1 max.	0.5 max.	1.0 max.	1.0 max.	0.3-1.0	1.0 max.
Cu		–	0.5 max	0.5 max.	–	–	–	0.5 max.
Si	0.2 max.	0.5	0.5 max.	0.5 max.	0.08 max.	1.0 max.	0.25-0.75	0.5 max.
Mo	7.0-9.5	0.5	–	–	15.0-17.0	8.0-10.0	1.0-3.0	–
Nb	2.75-4.0	2.0	0.7-1.2	2.5-3.5	–	–	–	0.7-1.2
Ti	1-1.7	1.8	2.0-2.6	0.1-0.4	–	–	–	2.25-2.75
Al	0.35 max	0.9	0.9-1.5	5.0-6.0	–	–	0.2-0.5	0.4-1.0
W		–	–	–	3-4.5	0.2-1	13-15	–
C	0.03 max.	0.03	0.1 max	0.03 max.		0.05-0.15	0.05-0.15	0.08 max.
Elastic modulus (GPa)	204	221	214	177.3	205	205	211.5	214
Yield strength (MPa)					Max 376	345	414	

Table 4 Variation of Inconel and Haynes alloys realized at Sapienza University.

		INCONEL				HAYNES		
Element	Density [Kg/m^3]	Inconel 600 % weigh	Variat. Nominal % weigh	Ni-A EDS analysis % weigh	Ni-B EDS analysis % weigh	Haynes 188 % weigh	Nominal % weigh	EDS % weigh
Fe	7860	6-10	6	6.1	6.2	Max 3		
Mo	10280		20	16.72	15.59			
W	19350					13-15	15	12.47
Cr	7140	14-17	13	13.43	12.97	21-23	22	23.75
Mn	7470					1.25		
Si	2330					0.2-0.5		
Cu	8960							
Ni	8908	Bal.	Bal.	63.87	65.06	20-24	22	24.71
Co	8900					Bal.	41	38.9
Density calculated with weight average			8890	8847	8811		10082	9772
Density measured experimentally on ingots				**8700**	**8700**			**9200**

5 Study on CCR type of glass.

Another aspect that had to be addressed during the design phase was the quality of the glass used for manufacturing CCRs for space application. The first rule for a glass to be used in space is to choose fused silica because of its transparency to ultraviolet (UV) light. However, there are several grades and classes of fused silica glass thus the need to check the possible different behavior of CCRs manufactured from different types of fused silica. The glass used on LARES CCRs is Suprasil 311 of Heraeus, while the one used for Edmund CCRs is Corning 7980 standard grade, homogeneity grade G, Class 0. Table 5 shows a comparison of the optical characteristics of Suprasil 311 and Corning 7980 and of Wavelength-Tech JGS1 fused silica CCRs. This last one was used for the CCRs installed on the TechnoSat satellite (now in orbit). The Wavelength-Tech JGS1 has been added for a comparison since the TechnoSat CCR array is made of 14 COTS CCRs for testing their performances on orbit. This last type of CCRs is to our knowledge not well characterized as it can be seen from Table 5.

5.1 UV interaction with CCR fused silica glass

Concerning the effect of neutral and charged particles, this is independent on the grade of the glass used, In fact, while the UV light, due to the high UV transparency of the glass, interacts only with the glass impurities, the particles practically interacts the same way with all the glass grades. The good behavior of the CCRs mounted on LAGEOS 1 in the last 43 years (since its launch) is an experimental proof that particle interaction with the CCR glasses is negligible in the time span of decades. The presence of inclusions and/or impurities could produce a variation of the refraction index of the fused silica probably due to volume variation of the inclusions induced by the UV interacting with the atoms of the inclusions [36]. The index of refraction therefore is not only a function of temperature but also of the number of defects (impurities and inclusions). According to the data reported in Table 5 the glass quality of Suprasil 311 is higher with respect to the quality of Corning 7980. Unfortunately, the factory of the COTS CCRs was not willing to change the material for the production. But even if the factory would agree it would be time consuming to optically qualify these new "specialty" CCRs that although geometrically identical, would be manufactured using a glass of different grade and class. It was thus decided to verify if the assumed lower quality of the glass used in Edmund CCRs was acceptable.

To further validate this conjecture we plotted in Figure 6 the transmittance as a function of impinging light wavelength. The data provided by the manufacturers have been plotted on the same graph. The two manufacturers do not state explicitly how the data are obtained: Heraeus stated that the transmittance curve for Suprasil 311 includes the Fresnel reflection loss (i.e. reflection losses at the interface between glass and air), while Corning did not provide any information about how they accounted for reflection loss when generating their curve. Therefore, to do a better comparison we added a third curve obtained by translating the Suprasil 311 original curve for discarding the effect of Fresnel loss. It is clear from Figure 6 that the transmittance curves are very similar. The high similarity of the curves confirms that the amount of impurities and inclusions (main cause of absorption of UV light) in the two fused silica glasses are similar.

[2] Equivalent to Suprasil 1 and 2 (Heraeus), Spectrosil A and B (Saint-Gobain) and Coming 7940 (Corning). Dynasil 1100 and 4100 (Dynasil), JGS1 is transparent in the ultraviolet and visible regions and has no absorption bands in 170-250 nm wavelength intervals. It has intensive OH absorption band in the interval of wavelength 2600-2800 nm. JGS1 is used for optics operating in the deep UV and the visible wavelength range (Laser Lenses, Windows, Prisms, Mirrors, etc.). It is practically free of bubbles and inclusions.

[3] COTS cube corner reflector made of Wavelength-Tech JGS1 have been installed on the TechnoSat satellite[34,35] .

[4] Not Specified. Next superior grade, grade F, has $\Delta n \leq 5 \times 10^{-6}$

[5] Defined as total cross-section in a 100 cm^3 volume, by ISO 10110-3

Table 5 Comparison of the characteristics of different fused silica.

	HERAEUS Suprasil 311	Corning 7980 • Standard Grade (attribute) • Grade G (homogeneity) • Class 0 (bubble and impurities)	WAVELENGTH-TECH JGS11.2[2],[3]
Homogeneity (Δn) PV (Peak to Valley)	$\leq 3 \times 10^{-6}$	NS[4]	NA
Inclusion, total cross-section[5] [mm^2]	$\leq$0.015	$\leq$0.03	NA
Inclusion, max size	0.08 mm	0.10 mm	NA
Metallic impurities [ppm]	Al $\leq$ 0.010 Ca $\leq$ 0.015 Cr $\leq$ 0.001 Cu $\leq$ 0.003 Fe $\leq$ 0.005 K $\leq$ 0.010 Li $\leq$ 0.001 Mg $\leq$ 0.005 Na $\leq$ 0.01 Ti $\leq$ 0.005 Total $\leq$ 0.065	≤ 1	≤ 5
Striae per ISO 10110-4	Class 5	Class 5	NA
Birefringence [nm/cm]	4.287 (PV)	≤ 5	2-4
OH		800-1000	1200
n @ 550 nm	1.4607	1.460076	1.46008
n @ 633nm	1.4570	1.457016	1.45702

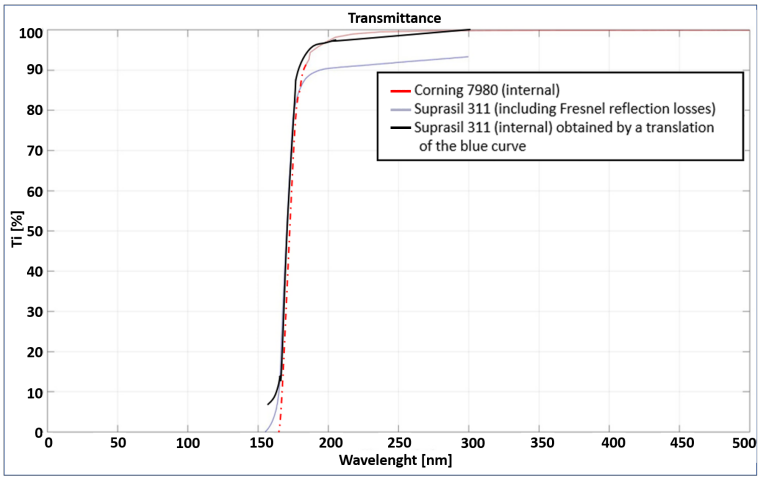

Fig. 6 Transmittance as a function of impinging light wavelength in different fused silica.

6 Material for the plastic rings

To avoid direct contact of the glass of the CCRs with the metal, two plastic rings shall be used. This will prevent cracks formation on the CCRs during handling and launch of the satellite. No critical issues have been identified for those components and therefore the LAGEOS and LARES proven design was considered acceptable for the material of the LARES 2 plastic rings. The material chosen is therefore the PCTFE (Polychlorotrifluoroethylene) commercialized at the time of LAGEOS as KEL-F by 3M and today with other trade names, depending on the manufacturer, such as Voltalef® (Arkema) or Neoflon™ (Daikin). This fluoropolymer has some favourable characteristics for the use in space and for this particular application such as: very broad temperature range of application from extremely low temperatures (-255 ^{o}C) up to +150 ^{o}C in continuous use (and up to + 200^{o}C as peak temperature), high mechanical resistance and in particular very low creep under compression, very high chemical inertness and low outgassing, excellent resistance to ultra-violet and X-ray radiation.

The main characteristics of this thermoplastic polymer are listed in Table 6

Table 6 Principal mechanical and thermal characteristics of PCTFE [37].

Density (Kg/m^3)	2110-2160
Elastic modulus (GPa)	1.4
Yield strength, at 23^{o}C (MPa)	34-50
Yield strength, at 120^{o}C(MPa)	3-6
Thermal conductivity (W/m K)	0.135
Specific heat (J/kg K)	900
Linear coefficient of thermal expansion, from -80^{o}C to +70^{o}C (K^{-1})	$5.5 \cdot 10^{-5}$
Linear coefficient of thermal expansion, from +70^{o}C to +150^{o}C (K^{-1})	$25 \cdot 10^{-5}$

7 Conclusions

The proper combination of the diameter of the satellite and the density of the alloy provides the best surface-to-mass ratio for LARES 2. A low value of this parameter is important to reduce the effect of non-conservative force perturbations on the measurement of frame-dragging. Also the material of the CCRs must show low sensitivity to ionizing radiation such as UV in order to guarantee long term durability of the CCRs. The paper describes the studies we performed on the materials for LARES 2 related to the aforementioned parameters.

Acknowledgements The authors acknowledge the support of the Italian Space Agency for the LARES and LARES 2 space missions under agreements No. 2017-23-H.0 and No.

2015-021-R.0. The authors thank Dr. F. Fraccaroli of Metalminotti s.r.l. for providing the 206 copper alloy. E. C. Pavlis acknowledges the support of NASA Grant NNX15AT34A. Special thanks to the International Laser Ranging Service (ILRS) for its willingness to track the future LARES 2 satellite and for distributing the laser ranging data to the scientific community.

References

1. Paolozzi, A., I. Ciufolini, E. Flamini, A. Gabrielli, S. Pirrotta, E. Mangraviti, A. Bursi, LARES in orbit: Some aspects of the mission (2012) Proceedings of the International Astronautical Congress, IAC, 6, pp. 4468-4474.
2. Ciufolini, I., Dragging of Inertial Frames, Nature, 449, 41-47 (2007).
3. Gurzadyan, V.G., I. Ciufolini, S. Sargsyan, G. Yegorian, S. Mirzoyan, A. Paolozzi, Satellite probing General Relativity and its extensions and Kolmogorov analysis (2013) EPL, 102 (6), art. no. 60002,
4. Pavlis, E.C., A. Paolozzi, G. Sindoni, I. Ciufolini, Contribution of LARES and geodetic satellites on environmental monitoring (2015) 2015 IEEE 15th International Conference on Environment and Electrical Engineering, EEEIC 2015 - Conference Proceedings, art. no. 7165479, pp. 1989-1994.
5. Ciufolini, I., Measurement of the Lense-Thirring drag on high-altitude laser-ranged artificial satellites, Phys. Rev. Lett. 56, 278-281 (1986).
6. Ciufolini, I., A Comprehensive Introduction to the LAGEOS Gravimetric Experiment, International Journal of Modern Physics A, 4, 3083-3145 (1989).
7. Ciufolini, I., A. Paolozzi, LARES: A New Laser-ranged satellite for fundamental physics and general relativity,Actual Problems of Aviation and Aerospace Systems 1, 61-73 21
8. Ciufolini, I., B.M. Monge, A. Paolozzi, R. Koenig, G. Sindoni, G. Michalak, E.C. Pavlis, Monte Carlo simulations of the LARES space experiment to test General Relativity and fundamental physics (2013) Classical and Quantum Gravity, 30 (23), art. no. 235009.
9. Ciufolini, I., E. C. Pavlis, A Confirmation of the General Relativistic Prediction of the Lense-Thirring Effect, Nature, 431, 958-960 (2004).
10. Ciufolini, I., E.C. Pavlis, J. Ries, R. Koenig, G. Sindoni, A. Paolozzi, H. Neumayer, Gravitomagnetism and its measurement with laser ranging to the LAGEOS satellites and GRACE Earth gravity models, in General Relativity and John Archibald Wheeler, vol. 367 (Springer Verlag GmbH, Berlino DEU), p. 371434 (2010)
11. Ciufolini, I., A. Paolozzi, E. C. Pavlis, R. Koenig, J. Ries, V. Gurzadyan, R. Matzner, R. Penrose, G. Sindoni, C. Paris, H. Khachatryan, S. Mirzoyan, A test of general relativity using the LARES and LAGEOS satellites and a GRACE Earth gravity model Measurement of Earth's dragging of inertial frames, Eur. Phys. J. C., 76:120 (2016) DOI 10.1140/epjc/s10052-016-3961-8
12. Thorne, K.S., R.H. Price, D.A. Macdonald, The Membrane Paradigm (Yale University Press, New Haven, 1986)
13. Ciufolini, I., Dragging of inertial frames. Nature 449, 41-47 (2007)
14. Ciufolini, I., J.A.Wheeler, Gravitation and Inertia (Princeton University Press, Princeton, 1995)
15. Misner, C.W., K.S. Thorne, J.A. Wheeler, Gravitation (Freeman, San Francisco, 1973).
16. Einstein, A. Letter to Ernst Mach. Zurich, 25 June 1913, in [15]. p544.
17. B.P. Abbott et al., Observation of gravitational waves from a binary black hole merger. Phys. Rev. Lett. 116, 061102 (2016)
18. Ciufolini, I., A. Paolozzi, E. C. Pavlis, G. Sindoni, R. Koenig, J. C. Ries, R. Matzner, V. Gurzadyan, R. Penrose, D. Rubincam and C. Paris, A new laser-ranged satellite for General Relativity and Space Geodesy. I. Introduction to the LARES 2 space experiment, Eur. Phys. J. Plus 132:336 (2017). https://doi.org/10.1140/epjp/i2017-11635-1
19. Ciufolini, I., E. C. Pavlis, G. Sindoni, J. C. Ries, A. Paolozzi, R. Koenig, C. Paris, A new laser-ranged satellite for General Relativity and Space Geodesy. II. Monte Carlo Simulations and covariance analyses of the LARES 2 Experiment, Eur. Phys. J. Plus 132:337 (2017).

20. Ciufolini,I., R. Matzner, V. Gurzadyan and R. Penrose, A new laser-ranged satellite for General Relativity and Space Geodesy. III. De Sitter effect and the LARES 2 space experiment, Eur. Phys. J. C 76:120 (2016) DOI 10.1140/epjc/s10052-016-3961-8 (2016).
21. Ciufolini,I., R. A. Matzner, J. Feng, A. Paolozzi, D. P. Rubincam, E. C. Pavlis, J. C. Ries, G. Sindoni, C. Paris, A new laser-ranged satellite for General Relativity and Space Geodesy. IV. Thermal drag and the LARES 2 space experiment, To appear in , Eur. Phys. J. Plus (2018).
22. Paolozzi, A., I. Ciufolini, C. Paris, G. Sindoni, LARES: A new satellite specifically designed for testing general relativity (2015) International Journal of Aerospace Engineering, 2015, art. no. 341384.
23. Paolozzi, A., I. Ciufolini, C. Vendittozzi, F. Passeggio, L. Caputo, G. Caputo, Technological challenges for manufacturing LARES satellite (2009) 60th International Astronautical Congress 2009, IAC 2009, 7, pp. 5925-5930.
24. Felli, F., A. Brotzu, D. Pilone, A. Paolozzi, I. Ciufolini, Fracture behavior of alloys for a new laser ranged satellite, Procedia Structural Integrity, Elsevier, 9 (2018) 295-302
25. Ciufolini, I., A. Paolozzi, C. Paris, G. Sindoni, The LARES satellite and its minimization of the thermal forces, (2014) 2014 IEEE International Workshop on Metrology for Aerospace, MetroAeroSpace 2014 - Proceedings, art. no. 6865938, pp. 299-303.
26. Paolozzi, A., I. Ciufolini, I. Peroni, C. Paris, M. Ramiconi,F.M. Onorati, L. Acquaroli, Testing the LARES separation system breadboards, (2009) 60th International Astronautical Congress 2009, IAC 2009, 10, pp. 8126-8131.
27. Paolozzi, A., I. Ciufolini, C. Vendittozzi, F. Felli, Material and surface properties of LARES satellite, (2012) Proceedings of the International Astronautical Congress, IAC, 8, pp. 6559-6565.
28. Paolozzi, A., I. Ciufolini, C. Caputo, L. Caputo, F. Passeggio, F.M. Onorati, C. Paris, A. Chiodo, LARES satellite and separation system (2012) Proceedings of the International Astronautical Congress, IAC, 9, pp. 6915-6922.
29. Paolozzi, A., I. Ciufolini, L. Schirone, I. Peroni, C. Paris, D. Spano, G. Sindoni, C. Vendittozzi, G. Battaglia, M. Ramiconi, Tests of LARES cube corner reflectors in simulated space environment (preliminary results),(2010) 61st International Astronautical Congress 2010, IAC 2010, 9, pp. 7390-7396.
30. Paolozzi, A., I. Ciufolini, C. Paris, G. Battaglia, N. Reinhart, Thermal tests on LARES satellite components,(2012) Proceedings of the International Astronautical Congress, IAC, 8, pp. 6653-6657.
31. http://www.specialmetalswiggin.co.uk/products/by-alloy/inconel
32. http://www.hightempmetals.com/techdata/hitempHaynes188data.php
33. Paolozzi, A., F. Felli, D. Pilone, A. Brotzu, I. Ciufolini, Development and analysis of a new alloy candidate for LARES 2 satellite. In: 69th International Astronautical Congress IAC 2018, Bremen 1-5 OCT 2018
34. https://ilrs.cddis.eosdis.nasa.gov/missions/satellite_missions/current_missions/tech_general.html
35. https://preview.tinyurl.com/tu-berlin-TechnoSat
36. Werneck., M.M., R.C.S.B. Allil, B.A.Ribeiro, F.B. de Nazaré, A Guide to Fiber Bragg Grating Sensors. Chapter from the book: Current Trends in Short and Long-period Fiber Grating. published by Intech. pag 14.15. 2013
37. Arkema Group, VOLTALEF® PCTFE technical brochure, 05/10/04.